

Special Issue:

Carbonaceous Aerosols in the
Atmosphere (II)

OPEN ACCESS 

Received: January 4, 2024

Revised: March 13, 2024

Accepted: March 20, 2024

*** Corresponding Authors:**


Longyi Shao
ShaoL@cumtb.edu.cn
Wenhua Wang
whwang91@126.com

Publisher:

Taiwan Association for Aerosol
Research

ISSN: 1680-8584 print

ISSN: 2071-1409 online

 **Copyright:** The Author(s).

This is an open access-article distributed under the terms of the [Creative Commons Attribution License \(CC BY 4.0\)](https://creativecommons.org/licenses/by/4.0/), which permits unrestricted use, distribution, and reproduction in any medium, provided the original author and source are cited.

Organic Carbon and Elemental Carbon in Two Dust Plumes at a Coastal City in North China

Wenhua Wang^{1,2*}, Hui Zhou^{1,2}, Ruihe Lyu³, Longyi Shao^{4*}, Wenmiao Li^{1,2}, Jiaoping Xing⁵, Zhe Zhao^{1,2}, Xian Li^{1,2}, Xiuyan Zhou^{1,2}, Daizhou Zhang⁶

¹School of Resources and Civil Engineering, Northeastern University, Shenyang 110819, China

²School of Resources and Materials, Northeastern University at Qinhuangdao, Qinhuangdao 066004, China

³College of Marine Resources and Environment, Hebei Normal University of Science and Technology, Qinhuangdao 066004, China

⁴State Key Laboratory of Coal Resources and Safe Mining and College of Geosciences and Surveying Engineering, China University of Mining and Technology, Beijing 100083, China

⁵School of Forestry, Jiangxi Agricultural University, Nanchang 330045, China

⁶Faculty of Environmental and Symbiotic Sciences, Prefectural University of Kumamoto, Kumamoto 862-8502, Japan

ABSTRACT

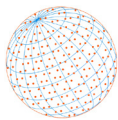
In the spring of 2023, two severe dust events occurred in the coastal city of Qinhuangdao, North China. We investigated organic carbon (OC) and elemental carbon (EC) in PM₁₀ using an OC/EC analyzer and identified the morphology and elemental composition of individual dust particles using a scanning electron microscope coupled with energy-dispersive X-ray (SEM-EDX). Results showed that OC mass concentrations varied significantly from 12.6 μg m⁻³ to 74.6 μg m⁻³ and showed a significant positive correlation with the PM₁₀ mass concentration. On average, OC made up 4.6% ± 1.1% and 4.3% ± 0.6% of the total PM₁₀ mass in two dust periods. Particularly, the weight ratio of OC-to-coarse particles (PM_{2.5-10}) was stable at approximately 2.8% ± 0.2%. In contrast, EC was less than 1.0% of the total PM₁₀ mass, with an average value of 0.13% ± 0.26% and 0.28% ± 0.15% in two dust periods. According to SEM-EDX results, the average weight ratios of sulfur on detected individual dust particles were 0.48% and 1.88% in two dust periods, which were less than the previously reported value in non-dust days, indicating inefficient formation of secondary species on the dust particles. SEM-EDX analysis further revealed that approximately 5.2% of the particles (in number) were irregularly shaped C-dominated particles, which might be carbonaceous species-containing particles. These results highlighted that the dust plumes brought a certain amount of OC but limited EC from dust sources.

Keywords: Dust storm, Organic carbon, Elemental carbon, Individual particle, SEM-EDX

1 INTRODUCTION

Dust storms originating from East Asian desert regions, such as the Gobi Desert in Mongolia and northwestern China, can travel thousands of kilometers, carrying a large number of dust particles into the atmosphere (Chen *et al.*, 2023). These dust storms contribute to approximately 20% of the global atmospheric dust load (Middleton, 2017). They can cause significant effects on climate and human health (Dimitriou and Kassomenos, 2019; Shi *et al.*, 2023). In the long-distance transport process, dust particles from East Asia can be transported to areas such as Korea, Japan, and the North Pacific Ocean (Kang *et al.*, 2013; Wang *et al.*, 2022), and can even be transported to the Arctic (Huang *et al.*, 2015).

Many previous studies have investigated the inorganic components of dust particles and discussed the heterogeneous reactions of dust particles during severe dust periods (Shao *et al.*, 2007;



Pan *et al.*, 2017; Li *et al.*, 2018; Feng *et al.*, 2023; Wang *et al.*, 2023). In addition to inorganic mineral particles, carbonaceous aerosols, including elemental carbon (EC) and organic carbon (OC) brought by severe dust, play a crucial role in the atmosphere (Wang *et al.*, 2012; Wen *et al.*, 2021; Liu *et al.*, 2023). These carbonaceous aerosols can exert a significant impact on human health and climate (Xu *et al.*, 2017; Hu *et al.*, 2020). However, the characteristics of carbonaceous aerosols transported by severe dust plumes have not been thoroughly understood. For instance, many previous studies collected samples either daily or during day/night intervals (Wu *et al.*, 2020; Ren *et al.*, 2021). Consequently, these samples might encompass aerosol particles before and after dust storms since dust storms usually last only a few hours (Wu *et al.*, 2017; Wen *et al.*, 2021), making it challenging to assess the carbonaceous concentrations of dust aerosols accurately.

In March and April 2023, North China, including the Beijing-Tianjin-Hebei region, experienced two intense dust storms, offering a valuable opportunity to investigate the physiochemistry of carbonaceous particles during dust periods. In this study, aerosol samples were collected to coincide with the onset and cessation of these dust storms. Subsequently, the “bulk chemical” composition was analyzed offline by using an OC/EC analyzer, which has been widely used in determining the concentrations of OC/EC in non-dust days. In addition, a scanning electron microscope coupled with energy-dispersive X-ray (SEM-EDX) was applied to analyze the detailed morphology and elemental composition of those individual dust particles.

2 EXPERIMENTAL

2.1 Sample Collection

Samples were collected on the 15th floor of a teaching building at Northeastern University in Qinhuangdao City (119.55°E, 39.92°N), as illustrated in Fig. 1. The sampling location was surrounded by traffic roads and residential areas, with no known significant large emission sources nearby,

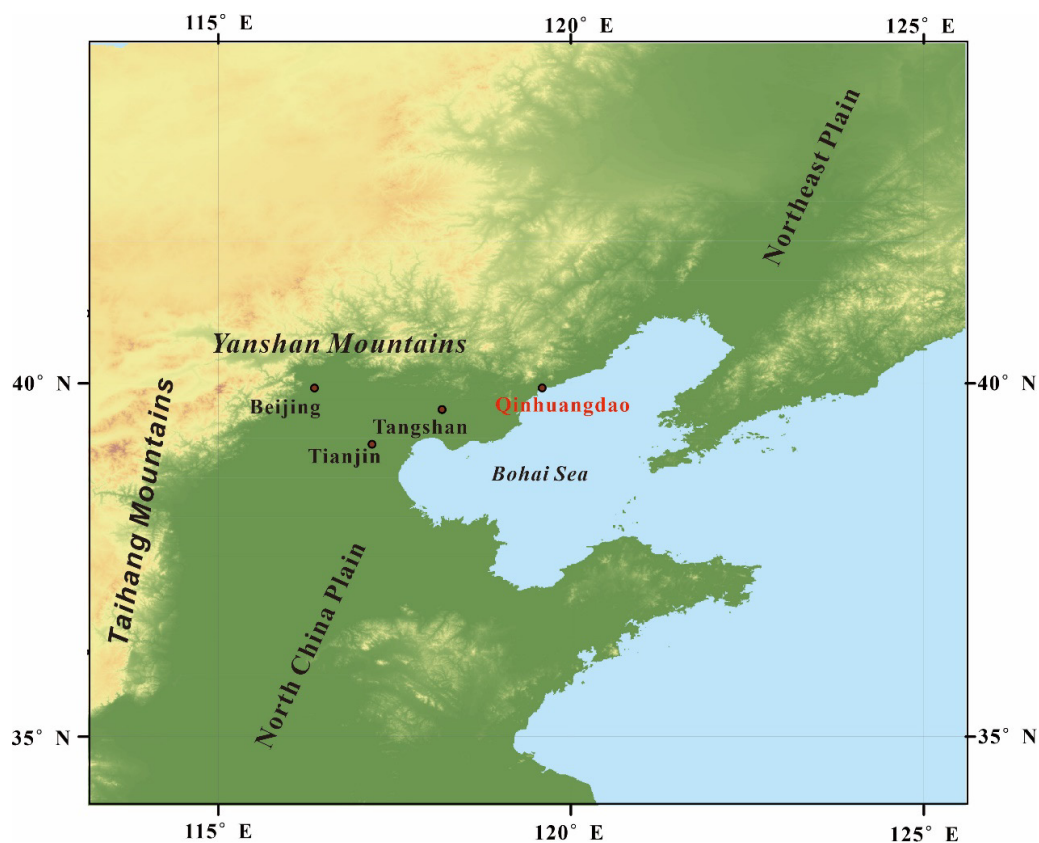
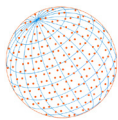


Fig. 1. Map showing the geographical locations of Qinhuangdao City.



such as power plant and industries. For “bulk chemical” analysis, the PM₁₀ samples were collected on quartz fiber filters (90 mm, Whatman QM-A) employing a medium-volume cascade sampler (100 L min⁻¹; Kingstar Electronic Technology Inc., China). PM_{2.5} samples were also simultaneously collected with the PM₁₀ during the second dust storm period. Two blank filters without opening the sampler for 4 hours were also collected. Detailed sample information can be seen in Table 1 and Fig. 2. Before collection, the quartz fiber filters were pretreated in a muffle furnace at 600°C for 4 hours to eliminate potential carbonaceous substances. After collection, those samples were sealed with foil bags and stored in a refrigerator (−15°C) to prevent volatilization and contamination. The quartz fiber filters were equilibrated with relative humidity (RH) of 50 ± 5% and temperature of 20 ± 1°C before being weighted. For individual particle analysis, the PM₁₀ samples were also collected on polycarbonate filters with a flow rate of 16.7 L min⁻¹. The sample information of individual particle samples can be seen in Table S1.

Table 1. Sampling information and mass concentrations of different chemical compositions.

Type	ID	Date (2023)	Sampling time	PM (μg m ⁻³)	OC (μg m ⁻³)	EC (μg m ⁻³)	OC/PM	EC/PM
Dust 1 (PM ₁₀)	Dust 1-1	3.22	10:30–13:30	958.7	28.9	0.12	3.01%	0.01%
	Dust 1-2	3.22	13:40–16:00	1762.6	62.5	0.02	3.55%	0.00%
	Dust 1-3	3.22	16:10–18:30	1684.0	74.6	0.02	4.43%	0.00%
	Dust 1-4	3.22	18:40–21:00	1619.7	66.6	0.02	4.11%	0.00%
	Dust 1-5	3.22	21:10–1:10 (+1)	1202.6	45.5	0.81	3.78%	0.07%
	Dust 1-6	3.23	2:00–6:00	415.2	18.9	0.00	4.56%	0.00%
	Dust 1-7	3.23	8:00–14:00	223.7	13.3	0.06	5.93%	0.03%
	Dust 1-8	3.23	15:00–21:00	226.5	12.6	0.43	5.57%	0.19%
	Dust 1-9	3.23	23:00–8:00 (+1)	203.9	13.4	1.69	6.58%	0.83%
		<i>Average</i>			921.9	37.4	0.35	4.61%
	<i>Std</i>			632.3	23.8	0.54	1.12%	0.26%
Dust 2 (PM ₁₀)	Dust 2-1	4.11	9:30–13:30	675.0	22.6	0.01	3.34%	0.00%
	Dust 2-2	4.12	8:00–13:50	350.0	15.2	1.09	4.35%	0.31%
	Dust 2-3	4.12	14:00–17:00	619.6	24.3	1.02	3.92%	0.17%
	Dust 2-4	4.12	17:40–21:30	519.8	20.7	1.11	3.99%	0.21%
	Dust 2-5	4.12	22:00–3:00 (+1)	536.7	28.0	1.75	5.21%	0.33%
	Dust 2-6	4.13	7:00–12:00	450.0	19.1	2.08	4.24%	0.46%
	Dust 2-7	4.13	12:40–21:00	298.0	14.9	1.33	5.01%	0.45%
		<i>Average</i>			492.7	20.7	1.20	4.29%
	<i>Std</i>			126.5	4.4	0.61	0.60%	0.15%
Dust 2 (PM _{2.5})	Dust 2-1	4.11	9:30–13:30	154.2	8.50	0.01	5.51%	0.01%
	Dust 2-2	4.12	8:00–13:50	97.2	8.01	0.86	8.24%	0.88%
	Dust 2-3	4.12	14:00–17:00	184.8	10.94	0.82	5.92%	0.44%
	Dust 2-4	4.12	17:40–21:30	163.0	11.00	0.90	6.75%	0.55%
	Dust 2-5	--	—	--	--	--	--	--
	Dust 2-6	4.13	7:00–12:00	120.0	10.76	1.43	8.97%	1.19%
	Dust 2-7	4.13	12:40–21:00	86.3	8.54	0.94	9.90%	1.09%
		<i>Average</i>			138.9	9.4	0.83	7.19%
	<i>Std</i>			35.0	1.3	0.39	1.73%	0.38%
Dust 2 (PM _{2.5-10}) ^a	Dust 2-1	4.11	9:30–13:30	520.8	14.05	0.00	2.70%	0.00%
	Dust 2-2	4.12	8:00–13:50	252.8	7.22	0.23	2.86%	0.09%
	Dust 2-3	4.12	14:00–17:00	434.8	13.36	0.20	3.07%	0.05%
	Dust 2-4	4.12	17:40–21:30	356.8	9.72	0.21	2.72%	0.06%
	Dust 2-5	--	—	--	--	--	--	--
	Dust 2-6	4.13	7:00–12:00	330.0	8.31	0.65	2.52%	0.20%
	Dust 2-7	4.13	12:40–21:00	211.8	6.40	0.39	3.02%	0.19%
		<i>Average</i>			351.2	9.8	0.28	2.82%
	<i>Std</i>			104.4	2.9	0.20	0.19%	0.07%

^a The value of PM_{2.5-10} was based on the calculation of PM₁₀ and PM_{2.5} value.

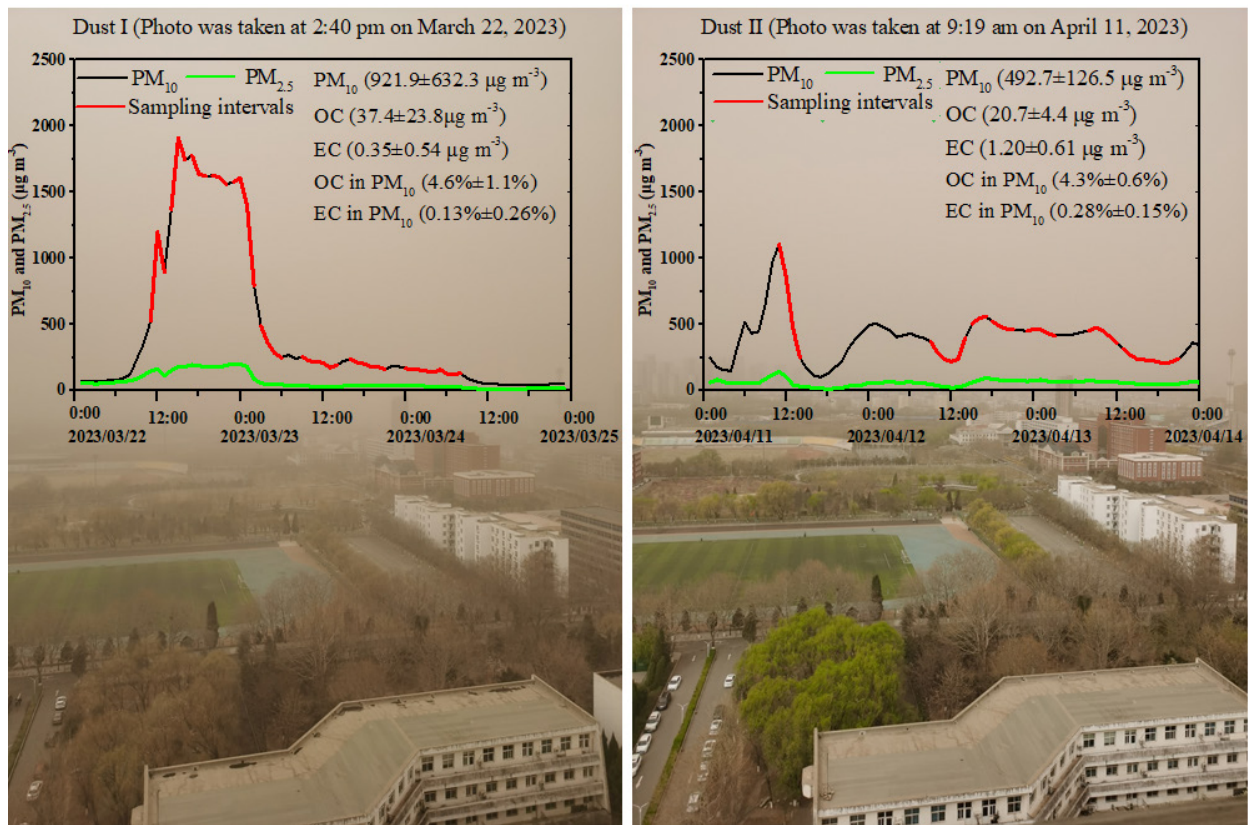
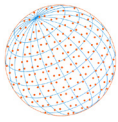


Fig. 2. Mass concentrations of PM₁₀ and sample information during severe dust periods (The background photos were taken during sampling periods).

2.2 Sample Analyses

Each filter was weighed at least three times before and after sampling to ensure reproducibility. The differences between the replicated weights were $< 10 \mu\text{g}$ per filter for blank filters and $< 20 \mu\text{g}$ for exposed samples. A $1.0 \times 1.5 \text{ cm}$ punch was removed from the quartz fiber filters for analysis using a Sunset Lab OC/EC analyzer (model 5L, USA) to determine the mass concentrations of OC and EC. This analyzer utilizes the thermal-optical transmittance (TOT) method recommended by the National Institute for Occupational Safety and Health (NIOSH). Before sample analysis, the analyzer was calibrated with sucrose. About 10% of aerosol samples were randomly selected and determined twice as the parallel samples. The relative deviations of the total carbon of the parallel samples were less than 10%. Field blank filters were also subjected to analysis, and the average value of the blank filter was $0.42 \mu\text{g cm}^{-2}$ for OC and $4.0 \times 10^{-4} \mu\text{g cm}^{-2}$ for EC. The average blank concentrations were subtracted from the sample results.

One patch of about 1 cm^2 of the polycarbonate filters was excised and affixed to the sample holder using conductive carbon tape. Subsequently, the particles were analyzed by using a scanning electron microscope (SEM) coupled with an energy-dispersive X-ray detector (FEI, Ltd., Hillsborough, USA).

3 RESULTS AND DISCUSSIONS

3.1 Characteristics of the Severe Dust Storm Episodes

Hourly averaged PM₁₀ and PM_{2.5} mass concentrations were obtained from the Chinese air quality online monitoring analysis platform's website (www.aqistudy.cn/). As shown in Fig. 2, the PM₁₀ mass concentrations exhibited a sharp increase starting at 9:00 (local time) on March 22, 2023, for the first dust storm and from 7:00 on April 11, 2023, for the second dust storm. During these severe dust periods, the ratios of PM_{2.5}/PM₁₀ were 0.09-0.21, significantly lower than those

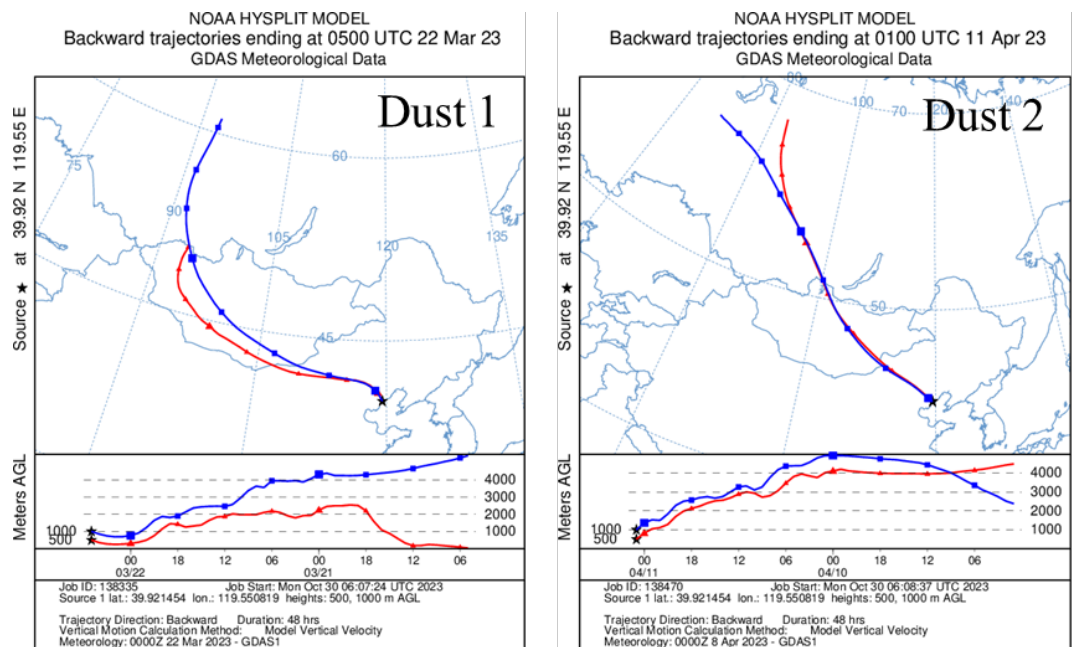
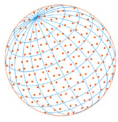


Fig. 3. 48-h backward trajectories of air masses arriving at the sampling site (39.92°N, 119.55°E) (https://www.ready.noaa.gov/HYSPLIT_traj.php).

observed before the dust storms (0.39–0.75). Fig. 2 also illustrates that the peak hourly averaged PM₁₀ mass concentration reached 1911 $\mu\text{g m}^{-3}$ during the first dust storm, whereas the value was 1107 $\mu\text{g m}^{-3}$ during the second dust storm. In addition, the high PM₁₀ mass concentrations lasted for a longer time in the first dust than in the second dust. The results indicated that the first dust storm impacted Qinhuangdao City more than the second dust.

To trace the sources of these severe dust storms, 48-hour backward trajectories of air masses were computed based on the on-line Hybrid Single-Particle Lagrangian Integrated Trajectory (HYSPLIT) model (Stein *et al.*, 2015; Rolph *et al.*, 2017). As shown in Fig. 3, both severe dust storms primarily originated from the Gobi Desert of Mongolia and northwestern China, although the first dust storm exhibited higher PM₁₀ mass concentrations than the second. Notably, previous research has indicated that the Gobi Desert in Mongolia contributed more than 42% of the Asian dust, surpassing the contribution from the Taklimakan Desert (26%) in March and April 2023 (Chen *et al.*, 2023). Therefore, the dust storms investigated in this study can be considered one of the important Asian dust storms.

3.2 EC Mass Concentrations during Dust Periods

EC, also known as black carbon (BC) for its typical sunlight-absorbing properties (Peng *et al.*, 2016; Pani *et al.*, 2020) or soot for its typical morphologies (Chen *et al.*, 2017; Zhang *et al.*, 2020; Shao *et al.*, 2022; Niu *et al.*, 2024), is composed of several C-bearing monomers under high-resolution SEM images as Fig. 4(a). EC primarily originates from the incomplete combustion of fossil fuels and biomass burning, making it one of the typical anthropogenic emissions (Fu and Chen, 2017; Ji *et al.*, 2019).

On average, EC mass concentrations accounted for $0.13\% \pm 0.26\%$ and $0.28\% \pm 0.15\%$ of the total PM₁₀ mass concentrations during the first and second dust storms, respectively. These values align with the findings from previous studies (Li *et al.*, 2023; Liu *et al.*, 2023). For example, Liu *et al.* (2023) found EC mass concentrations in PM_{2.5} was 0.2 $\mu\text{g m}^{-3}$, constituting 0.14% of the total PM_{2.5} during severe dust periods in Beijing. In addition, recent studies conducted in Wuhai, a city near the dust sources in northwestern China, indicated that EC accounted for 0.3%–0.5% of the total PM_{2.5} mass concentrations during two severe dust storm periods with averaged PM_{2.5} mass concentrations 252 $\mu\text{g m}^{-3}$ (Li *et al.*, 2023). These findings suggested that EC only comprises a small fraction of the total PM₁₀ during severe dust periods.

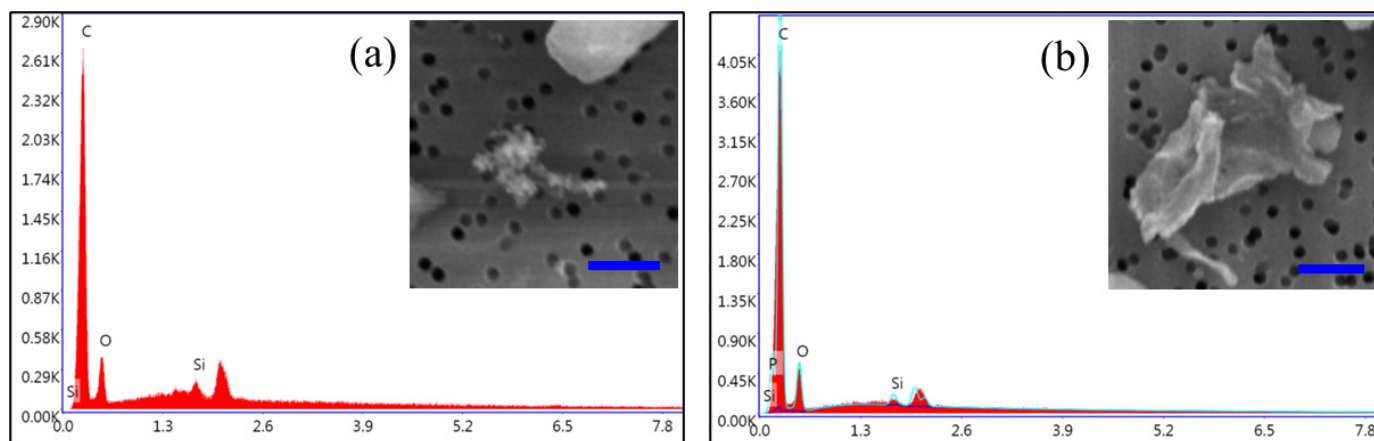
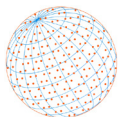


Fig. 4. High-resolution images of carbonaceous particles and their corresponding elemental compositions (scale bar: 1 μm). (a) is a soot particle and (b) is an organic particle.

During the onset of severe dust events, both the mass concentrations of EC and their corresponding mass ratios to the PM_{10} were lower than those observed at the end of the severe dust events, as indicated in Table 1. This observation is in line with the understanding that EC was mainly from anthropogenic emissions rather than dust sources and the anthropogenic emissions can be diluted by the severe dust storms (Wang *et al.*, 2012; Liu *et al.*, 2023).

3.3 OC Mass Concentrations during Dust Periods

In this study, OC mass concentrations ranged from $12.6 \mu\text{g m}^{-3}$ to $74.6 \mu\text{g m}^{-3}$ with an average value of $37.4 \mu\text{g m}^{-3}$ in the first dust periods and ranged from $14.9 \mu\text{g m}^{-3}$ to $28.0 \mu\text{g m}^{-3}$ with an average value of $20.7 \mu\text{g m}^{-3}$ in the second dust periods. Previous studies have also observed higher proportions of OC mass concentrations in PM during severe dust periods (Wang *et al.*, 2012; Liu *et al.*, 2014; Wen *et al.*, 2021; Li *et al.*, 2023; Liu *et al.*, 2023; Xu *et al.*, 2023). For example, Liu *et al.* (2014) reported higher OC mass concentrations in PM_{10} in Beijing during severe dust periods ($34.82 \mu\text{g m}^{-3}$) than non-dust periods ($21.72 \mu\text{g m}^{-3}$), suggesting regional transport source instead of local emissions affected the air more during severe dust periods. Liu *et al.* (2023) similarly found higher OC mass concentrations in $\text{PM}_{2.5}$ on dusty days ($13.4 \mu\text{g m}^{-3}$) than the average of whole sampling periods including haze and non-haze days ($9.1 \mu\text{g m}^{-3}$) in Beijing.

Although OC mass concentrations varied significantly, their proportions to PM remained relatively stable. The mass ratios of OC-to- PM_{10} ranged from 3.0% to 6.6% during the first dust storm and ranged from 3.3% to 5.2% during the second dust storm as shown in Table 1. In addition, the average values of the OC to PM_{10} were very similar between the first ($4.6\% \pm 1.1\%$) and second ($4.3\% \pm 0.6\%$) dust storms. Further analysis revealed a linear correlation between OC mass concentrations and PM_{10} mass concentrations, as shown in Fig. 5 ($n = 16$, $R = 0.976$). The results suggested that during severe dust periods, the OC might be mainly from the dust sources.

It is known that the small-sized secondary OC can be formed in the atmosphere, and the anthropogenic emitted OC tends to have less particle size (Guo *et al.*, 2014b). To further explore the possible sources of OC during severe dust periods, the $\text{PM}_{2.5}$ samples were simultaneously collected alongside the PM_{10} during the second dust period. It should be mentioned that due to a manual error, a pair of $\text{PM}_{2.5}$ and PM_{10} were not collected simultaneously (ID: "Dust 2-5"). The OC-to- $\text{PM}_{2.5}$ mass ratios ranged from 5.5% to 9.9%, higher than that of OC-to- PM_{10} mass ratios (2.5%–3.1%). Therefore, we can infer there might be less secondary organic aerosol formation on large-size particles. In addition, OC-to- PM_{10} mass ratios were relatively stable but their mass concentrations varied. The results confirmed that OC in coarse particles might be mainly from dust sources. SEM-EDX analysis showed the weight ratios of sulfur on individual mineral dust were only 0.48% and 1.88%, much lower than the previous reported value (11.0%) on non-dust day (Wang 2020), further supporting limited secondary aerosol formation as shown in Fig. 6. In addition, we found there were 5.2% (in number) of irregular shaped C-dominated particles (Fig. 4(b)) based

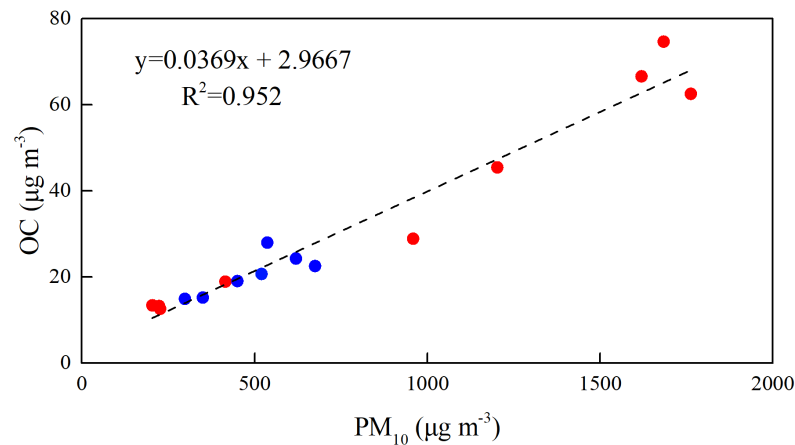
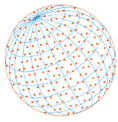


Fig. 5. Correlations of PM₁₀ and organic carbon (OC) during two severe dust storm periods. The red dots represent the samples collected during the first dust storm periods (22–24 March 2023) and the blue dots the second (11–13 April 2023).

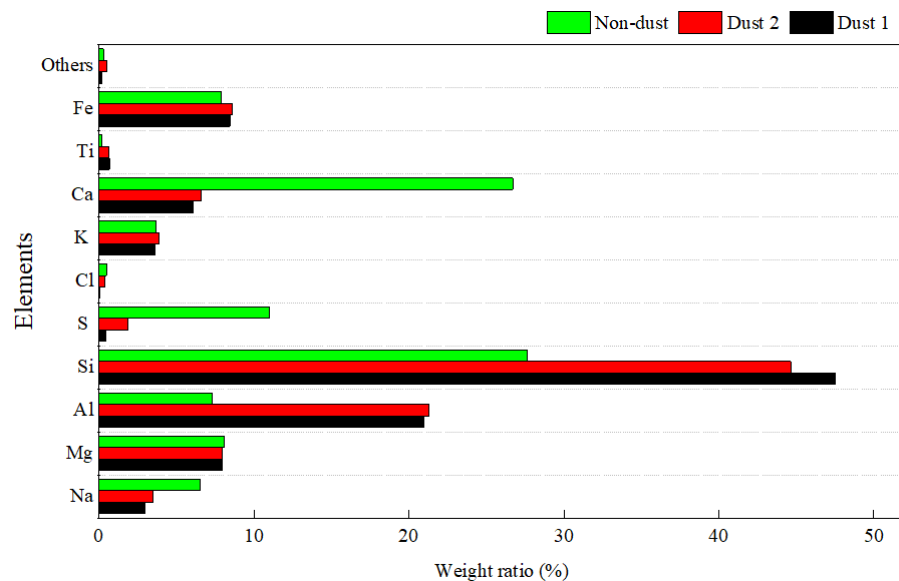
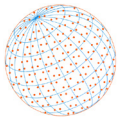


Fig. 6. Relative weight ratios of different elements on individual mineral particles during two severe dust periods (non-dust data was based on Wang (2020)).

on the SEM-EDX results. These findings collectively suggested that OC and EC might originate from distinct sources, with OC being more closely associated with dust sources and EC associated with anthropogenic emissions.

3.4 Atmospheric Implications

Understanding the characteristics of carbonaceous aerosols during severe dust periods holds significant implications for the atmosphere. It is well known that OC comprises both primary and secondary types (Guo *et al.*, 2014b; Chen *et al.*, 2017; Ji *et al.*, 2019). A previously introduced method, the EC tracer method, has been used to estimate the formation of secondary organic aerosols (Xu *et al.*, 2023). The key step of this method is to determine the primary OC/EC ratio in the study period and region. Previous studies have applied the minimum value of OC/EC during sampling periods as the primary OC/EC ratio (Guo *et al.*, 2014a; Xu *et al.*, 2023). However, the method has an assumption that OC and EC were emitted from similar sources during the study periods. Our results suggested that OC and EC might originate from different sources, with OC being



more closely associated with dust sources and EC associated with anthropogenic emissions during severe dust periods. Therefore, the primary OC/EC ratios might be higher during severe dust periods than non-dust periods. For example, the average values of OC/EC were 35.4 and 15.4, respectively, for two dust periods in this study, higher than the average value of OC/EC on non-dust days in surrounding Beijing-Tianjin-Tangshan regions (1.2–11.4) (Ji *et al.*, 2019). Therefore, different OC/EC tracers should be applied when samples were both collected during dust and non-dust periods, otherwise the secondary organic aerosols during dust periods might be overestimated (Xu *et al.*, 2023).

4 CONCLUSIONS

Two severe dust storms originating from the desert regions in Mongolia and northwestern China invaded North China. This study analyzed OC and EC mass concentrations, as well as the morphologies of individual particles at the coastal city of Qinhuangdao during two dust periods. The results showed OC mass concentrations varied significantly but were well correlated with the PM₁₀ mass concentrations. On average, OC made up $4.6\% \pm 1.1\%$ and $4.3\% \pm 0.6\%$ of the total PM₁₀ mass in two dust periods. In contrast, EC was less than 1.0% of the total PM₁₀ mass, with an average value of $0.13\% \pm 0.26\%$ and $0.28\% \pm 0.15\%$ in two dust periods. In addition, there were 5.2% (in number) of irregularly shaped C-dominated particles, and that the mineral particles contained limited sulfur content according to the SEM-EDX results. The research highlighted that the severe dust plumes transported not only mineral dust but also some OC to downstream areas, with OC estimated at 2.8 wt.% of coarse particles (PM_{2.5-10}).

Although the research provides some interesting results based on the filter-based OC and EC concentrations during severe dust periods, it should be mentioned that the heavy loading of dust might impact the TOT analysis due to pyrolysis, inorganic carbon, and laser transmittance. In addition, this study only analyzed the concentrations of OC and EC. More detailed information such as water-soluble organic species should be investigated in future research to understand the carbonaceous component during severe dust periods fully. This study only analyzed limited number of dust samples since the dust storm lasted for a short time. Therefore, more dust samples from different dust periods should be collected and analyzed in further research.

ACKNOWLEDGMENT

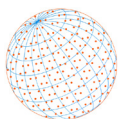
This work was supported by the Natural Science Foundation of Hebei Province (B2022407001 and D2021501004), the National Natural Science Foundation of China (42075107 and 42065007), and Fundamental Research Funds for the Central Universities (N2223011).

SUPPLEMENTARY MATERIAL

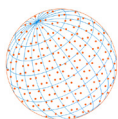
Supplementary material for this article can be found in the online version at <https://doi.org/10.4209/aaqr.240002>

REFERENCES

- Chen, J., Li, C., Ristovski, Z., Milic, A., Gu, Y., Islam, M.S., Wang, S., Hao, J., Zhang, H., He, C., Guo, H., Fu, H., Miljevic, B., Morawska, L., Thai, P., Lam, Y.F., Pereira, G., Ding, A., Huang, X., Dumka, U.C. (2017). A review of biomass burning: Emissions and impacts on air quality, health and climate in China. *Sci. Total Environ.* 579, 1000–1034. <https://doi.org/10.1016/j.scitotenv.2016.11.025>
- Chen, S., Zhao, D., Huang, J., He, J., Chen, Y., Chen, J., Bi, H., Lou, G., Du, S., Zhang, Y., Yang, F. (2023). Mongolia contributed more than 42% of the dust concentrations in Northern China in March and April 2023. *Adv. Atmos. Sci.* 40, 1549–1557. <https://doi.org/10.1007/s00376-023-3062-1>



- Dimitriou, K., Kassomenos, P. (2019). Estimation of North African dust contribution on PM₁₀ episodes at four continental Greek cities. *Ecological Indicators* 106, 105530. <https://doi.org/10.1016/j.ecolind.2019.105530>
- Feng, X., Shao, L., Jones, T., Li, Y., Zhang, M., Ge, S., Cao, Y., BéruBé, K., Zhang, D. (2023). The changing sulphur content of a northern Chinese dust storm: Initiation, attenuation and culmination. *Atmos. Environ.* 297, 119606. <https://doi.org/10.1016/j.atmosenv.2023.119606>
- Fu, H., Chen, J. (2017). Formation, features and controlling strategies of severe haze-fog pollutions in China. *Sci. Total Environ.* 578, 121–138. <https://doi.org/10.1016/j.scitotenv.2016.10.201>
- Guo, S., Hu, M., Guo, Q., Shang, D. (2014a). Comparison of secondary organic aerosol estimation methods. *Acta Chim. Sinica* 72, 658. <https://doi.org/10.6023/A14040254>
- Guo, S., Hu, M., Zamora, M.L., Peng, J., Shang, D., Zheng, J., Du, Z., Wu, Z., Shao, M., Zeng, L., Molina, M.J., Zhang, R. (2014b). Elucidating severe urban haze formation in China. *Proc. Natl. Acad. Sci. U.S.A.* 111, 17373–17378. <https://doi.org/10.1073/pnas.1419604111>
- Hu, W., Murata, K., Fan, C., Huang, S., Matsusaki, H., Fu, P., Zhang, D. (2020). Abundance and viability of particle-attached and free-floating bacteria in dusty and nondusty air. *Biogeosciences* 17, 4477–4487. <https://doi.org/10.5194/bg-17-4477-2020>
- Huang, Z., Huang, J., Hayasaka, T., Wang, S., Zhou, T., Jin, H. (2015). Short-cut transport path for Asian dust directly to the Arctic: a case study. *Environ. Res. Lett.* 10, 114018. <https://doi.org/10.1088/1748-9326/10/11/114018>
- Ji, D., Gao, M., Maenhaut, W., He, J., Wu, C., Cheng, L., Gao, W., Sun, Y., Sun, J., Xin, J., Wang, L., Wang, Y. (2019). The carbonaceous aerosol levels still remain a challenge in the Beijing-Tianjin-Hebei region of China: Insights from continuous high temporal resolution measurements in multiple cities. *Environ. Int.* 126, 171–183. <https://doi.org/10.1016/j.envint.2019.02.034>
- Kang, E., Han, J., Lee, M., Lee, G., Kim, J.C. (2013). Chemical characteristics of size-resolved aerosols from Asian dust and haze episode in Seoul Metropolitan City. *Atmos. Res.* 127, 34–46. <https://doi.org/10.1016/j.atmosres.2013.02.002>
- Li, J., Shao, L., Chang, L., Xing, J., Wang, W., Li, W., Zhang, D. (2018). Physicochemical Characteristics and Possible Sources of Individual Mineral Particles in a Dust Storm Episode in Beijing, China. *Atmosphere* 9, 269. <https://doi.org/10.3390/atmos9070269>
- Li, R., Zhang, Miao, Du, Y., Wang, G., Shang, C., Liu, Y., Zhang, Min, Meng, Q., Cui, M., Yan, C. (2023). Impacts of dust events on chemical characterization and associated source contributions of atmospheric particulate matter in northern China. *Environ. Pollut.* 316, 120597. <https://doi.org/10.1016/j.envpol.2022.120597>
- Liu, Q., Liu, Y., Yin, J., Zhang, M., Zhang, T. (2014). Chemical characteristics and source apportionment of PM₁₀ during Asian dust storm and non-dust storm days in Beijing. *Atmos. Environ.* 91, 85–94. <https://doi.org/10.1016/j.atmosenv.2014.03.057>
- Liu, T., Duan, F., Ma, Y., Ma, T., Zhang, Qinqin, Xu, Y., Li, F., Huang, T., Kimoto, T., Zhang, Qiang, He, K. (2023). Classification and sources of extremely severe sandstorms mixed with haze pollution in Beijing. *Environ. Pollut.* 322, 121154. <https://doi.org/10.1016/j.envpol.2023.121154>
- Middleton, N.J. (2017). Desert dust hazards: A global review. *Aeolian Res.* 24, 53–63. <https://doi.org/10.1016/j.aeolia.2016.12.001>
- Niu, H., Wu, C., Ma, X., Ji, X., Tian, Y., Wang, J. (2024). Evaluation of single particle morphological characteristics and human health risks in different functional areas. *World J. Eng.* <https://doi.org/10.1108/WJE-08-2023-0310>
- Pan, X., Uno, I., Wang, Z., Nishizawa, T., Sugimoto, N., Yamamoto, S., Kobayashi, H., Sun, Y., Fu, P., Tang, X., Wang, Z. (2017). Real-time observational evidence of changing Asian dust morphology with the mixing of heavy anthropogenic pollution. *Sci. Rep.* 7, 335. <https://doi.org/10.1038/s41598-017-00444-w>
- Pani, S.K., Wang, S.H., Lin, N.H., Chantara, S., Lee, C.T., Thepnuan, D. (2020). Black carbon over an urban atmosphere in northern peninsular Southeast Asia: Characteristics, source apportionment, and associated health risks. *Environ. Pollut.* 259, 113871. <https://doi.org/10.1016/j.envpol.2019.113871>
- Peng, J., Hu, M., Guo, S., Du, Z., Zheng, J., Shang, D., Levy Zamora, M., Zeng, L., Shao, M., Wu, Y.S., Zheng, Jun, Wang, Y., Glen, C.R., Collins, D.R., Molina, M.J., Zhang, R. (2016). Markedly enhanced absorption and direct radiative forcing of black carbon under polluted urban



- environments. *Proc. Natl. Acad. Sci. U.S.A.* 113, 4266–4271. <https://doi.org/10.1073/pnas.1602310113>
- Ren, Y., Wei, J., Wu, Z., Ji, Y., Bi, F., Gao, R., Wang, X., Wang, G., Li, H. (2021). Chemical components and source identification of PM_{2.5} in non-heating season in Beijing: The influences of biomass burning and dust. *Atmos. Res.* 251, 105412. <https://doi.org/10.1016/j.atmosres.2020.105412>
- Rolph, G., Stein, A., Stunder, B. (2017). Real-time Environmental Applications and Display sYstem: READY. *Environ. Modell. Software* 95, 210–228. <https://doi.org/10.1016/j.envsoft.2017.06.025>
- Shao, L., Li, W., Yang, S., Shi, Z., Lü, S. (2007). Mineralogical characteristics of airborne particles collected in Beijing during a severe Asian dust storm period in spring 2002. *Sci. China Ser. D* 50, 953–959. <https://doi.org/10.1007/s11430-007-0035-7>
- Shao, L., Liu, P., Jones, T., Yang, S., Wang, W., Zhang, D., Li, Y., Yang, C.X., Xing, J., Hou, C., Zhang, M., Feng, X., Li, W., Bérubé, K. (2022). A review of atmospheric individual particle analyses: Methodologies and applications in environmental research. *Gondwana Res.* 110, 347–369. <https://doi.org/10.1016/j.gr.2022.01.007>
- Shi, C., Mao, R., Gong, D.Y., Kim, S.J., Feng, X., Sun, Y., Dong, H. (2023). Increased dust transport from Patagonia to eastern Antarctica during 2000–2020. *Global Planet. Change* 227, 104186. <https://doi.org/10.1016/j.gloplacha.2023.104186>
- Stein, A.F., Draxler, R.R., Rolph, G.D., Stunder, B.J.B., Cohen, M.D., Ngan, F. (2015). NOAA's HYSPLIT atmospheric transport and dispersion modeling system. *Bull. Am. Meteorol. Soc.* 96, 2059–2077. <https://doi.org/10.1175/BAMS-D-14-00110.1>
- Wang, G.H., Li, J.J., Cheng, C.L., Zhou, B.H., Xie, M.J., Hu, S.Y., Meng, J.J., Sun, T., Ren, Y.Q., Cao, J.J., Liu, S.X., Zhang, T., Zhao, Z.Z. (2012). Observation of atmospheric aerosols at Mt. Hua and Mt. Tai in central and east China during spring 2009 - Part 2: Impact of dust storm on organic aerosol composition and size distribution. *Atmos. Chem. Phys.* 12, 4065–4080. <https://doi.org/10.5194/acp-12-4065-2012>
- Wang, W. (2020). Physico-chemical characteristics and aging process of single particles with different PM_{2.5} mass level in urban Beijing [D]. China University of Mining and Technology, China.
- Wang, W., Shao, L., Zhang, D., Li, Y., Li, W., Liu, P., Xing, J. (2022). Mineralogical similarities and differences of dust storm particles at Beijing from deserts in the north and northwest. *Sci. Total Environ.* 803, 149980. <https://doi.org/10.1016/j.scitotenv.2021.149980>
- Wang, W., Shao, L., Li, X., Li, Y., Lyu, R., Zhou, X. (2023). Changes of water-soluble inorganic sulfate and nitrate during severe dust storm episodes in a coastal city of North China. *Environ. Pollut.* 335, 122288. <https://doi.org/10.1016/j.envpol.2023.122288>
- Wen, H., Zhou, Y., Xu, X., Wang, T., Chen, Q., Chen, Q., Li, W., Wang, Z., Huang, Z., Zhou, T., Shi, J., Bi, J., Ji, M., Wang, X. (2021). Water-soluble brown carbon in atmospheric aerosols along the transport pathway of Asian dust: Optical properties, chemical compositions, and potential sources. *Sci. Total Environ.* 789, 147971. <https://doi.org/10.1016/j.scitotenv.2021.147971>
- Wu, C., Zhang, S., Wang, G., Lv, S., Li, D., Liu, L., Li, J., Liu, S., Du, W., Meng, J., Qiao, L., Zhou, M., Huang, C., Wang, H. (2020). Efficient heterogeneous formation of ammonium nitrate on the saline mineral particle surface in the atmosphere of East Asia during dust storm periods. *Environ. Sci. Technol.* 54, 15622–15630. <https://doi.org/10.1021/acs.est.0c04544>
- Wu, F., Zhang, D., Cao, J., Guo, X., Xia, Y., Zhang, T., Lu, H., Cheng, Y. (2017). Limited production of sulfate and nitrate on front-associated dust storm particles moving from desert to distant populated areas in northwestern China. *Atmos. Chem. Phys.* 17, 14473–14484. <https://doi.org/10.5194/acp-17-14473-2017>
- Xu, G., Stegmann, P.G., Brooks, S.D., Yang, P. (2017). Modeling the single and multiple scattering properties of soot-laden mineral dust aerosols. *Opt. Express* 25, A990. <https://doi.org/10.1364/OE.25.00A990>
- Xu, K., Liu, Y., Li, C., Zhang, C., Liu, X., Li, Q., Xiong, M., Zhang, Y., Yin, S., Ding, Y. (2023). Enhanced secondary organic aerosol formation during dust episodes by photochemical reactions in the winter in Wuhan. *J. Environ. Sci.* 133, 70–82. <https://doi.org/10.1016/j.jes.2022.04.018>
- Zhang, J., Liu, L., Xu, L., Lin, Q., Zhao, H., Wang, Z., Guo, S., Hu, M., Liu, D., Shi, Z., Huang, D., Li, W. (2020). Exploring wintertime regional haze in northeast China: role of coal and biomass burning. *Atmos. Chem. Phys.* 20, 5355–5372. <https://doi.org/10.5194/acp-20-5355-2020>